Hydrodynamic Stability of Marangoni Films:

II. A Preliminary Analysis of the Effect of Interphase Mass Transfer

K. H. WANG, V. LUDVIKSSON, and E. N. LIGHTFOOT

Department of Chemical Engineering
University of Wisconsin, Madison, Wisconsin 53706

The stability of vertical laminar falling films subjected to interphase mass transfer and surface-tension gradients in the direction of flow is investigated by linear perturbation analysis. The perturbations considered are vertical waves or rivulets as described by Ludviksson and Lightfoot for nonisothermal films. Perturbations of this type are thought to lead to the maldistribution of flow observed in distillation and gas absorption by Zuiderweg and Harmens and by Francis and Berg.

Three unstable regions are predicted, one corresponding closely to that found by Ludviksson and Lightfoot, and two new ones, previously unreported, resulting from interphase mass transfer across the free surface.

These predictions confirm the conclusions of Zuiderweg and Harmens for situations in which surface tension increases upward, and they provide a means of estimating the range of unstable gradients. Experimental evidence for instability predicted when the surface tension increases downward is inconclusive. Further investigation of this region, which is of considerable importance, is recommended.

The importance of surface-tension gradients in mass transfer across mobile interfaces has long been recognized, and considerable research effort has been devoted to characterizing surface-tension-driven flows. Some experimental observations on liquid thin film have been reported in which mass transfer coefficients are severalfold higher than for flat films (*4* to *6*), reportedly because of interfacial turbulence resulting from surface-tension gradients. In other cases observations of film breakup and correspondingly poor mass transfer operations have been reported. These include the absorption of ethanol vapor (*7*) and ammonia (*8, 9*) into thin aqueous films and the distillation of binary mixture (*10*). Zuiderweg and Harmens (*2*) have tried to correlate the observed interfacial behavior qualitatively with the performance efficiency of some distillation columns for several mixtures.

Considerably less work has been done on trying to predict interfacial turbulence and its influence on mass transfer from theoretical analysis of the equations of change. Some success, however, has been gained from analyzing interfacial turbulence by the methods of linear stability theory. Thus the pioneering paper of Sternling and Scriven (*11*) has given valuable insight into the complicated interfacial phenomena often observed in liquid-liquid extraction.

Recently Ludviksson and Lightfoot (*1*) have analyzed the hydrodynamic stability of a vertical laminar film subject to upward directed surface-tension gradients induced by temperature gradients. It is the purpose of this paper to attempt a simliar analysis for the corresponding mass transfer problem previously investigated experimentally by Zuiderweg and Harmens: distillation or absorption in wetted-wall columns. In such operations one would expect a surface-tension gradient to develop along the column, directed either upward or downward, and that subsequent disturbances to the local film thickness could lead to growing rivulets or drops of liquid running down the walls, much like the pictures of channeling shown by Zuiderweg and Harmens.

This analysis will follow very closely the analysis of Ludviksson and Lightfoot with the organization and notations kept the same as much as possible for the convenience of the reader. The equations are presented with minimum discussion when such analogy is complete.

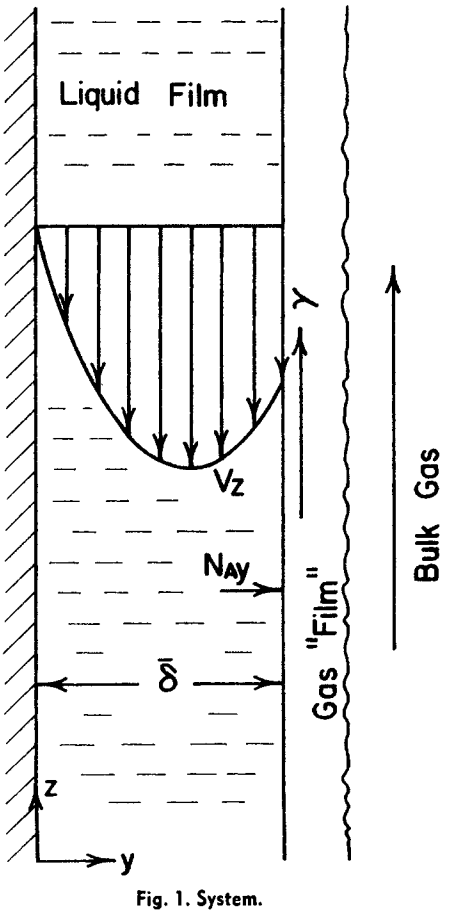

Fig. 1. System.

DESCRIPTION OF THE UNPERTURBED SYSTEM

The unperturbed system is indicated schematically in Figure 1. It consists of a section of column in which the film thickness is very small compared to the column diameter such that one can neglect the column curvature effects. We assume that the liquid is in steady nonrippling laminar flow down a flat vertical plate. We consider a section of column short enough such that we have a constant mass flux across the gas-liquid interface, and we assume that the gas phase is in turbulent flow such that its concentration is a linear function of z only:

$$\overline{Y}_A = K\overline{G}_0 z + \overline{Y}_{A0} \tag{1}$$

This situation will be closely approximated in distillation at total reflux for intermediate concentration ranges. Under these conditions it follows that

$$\text{At } y = 0 \quad \frac{\partial \overline{X}_A}{\partial y} = 0 \tag{2}$$

$$\text{At } y = \overline{\delta} \quad \overline{N}_{Ay} = -\overline{c}_L \mathcal{D}_{AL} \frac{\partial \overline{X}_A}{\partial y} = \overline{c}_g k_c (K\overline{X}_A - \overline{Y}_A) \tag{3}$$

Here the total concentration $\overline{c}$ is assumed constant. As a requirement of Equation (3) and constant mass flux assumptions, we obtain a linear dependence of liquid phase concentration on z:

$$\overline{X}_A = \overline{G}_0 z + \overline{f}(y) \tag{4}$$

We now further assume that all physical and transport properties are constant except that the surface tension is a function of surface composition in the liquid such that

$$\gamma = \frac{\partial \sigma}{\partial z} = \Gamma \overline{G}_0 \tag{5}$$

Here Γ, the rate of change of surface tension with concentration, is assumed to be constant. Then the velocity profiles are the same as for the development of Ludviksson and Lightfoot, namely

$$\overline{V}_x = \overline{V}_y = 0 \tag{6}$$

$$\overline{V}_z = \left(\frac{\gamma\overline{\delta}}{\mu}\right)\eta - \left(\frac{\rho g \overline{\delta}^2}{\mu}\right)\left(\eta - \frac{\eta^2}{2}\right) \tag{7}$$

To obtain $\overline{f}(y)$, we substitute Equation (4) into the equation of continuity for species A:

$$V_z \frac{\partial \overline{X}_A}{\partial z} = \mathcal{D}_{AL} \frac{\partial^2 \overline{X}_A}{\partial y^2} \tag{8}$$

and solve it with Equations (2) and (3) as boundary conditions. The complete expression for concentration is then

$$\overline{X}_A = \overline{G}_0 z + \frac{\overline{G}_0 \overline{\delta}^3}{\mu \mathcal{D}_{AL}} \left[(\gamma - \rho g \overline{\delta}) \frac{\eta^3}{6} + \rho g \overline{\delta} \frac{\eta^4}{24} \right] + \frac{\overline{G}_0 \overline{\delta}^3}{\mu \mathcal{D}_{AL}} \left[\frac{\rho g \overline{\delta}}{8} - \frac{\gamma}{6} \right] + \frac{\overline{c}_L \overline{G}_0 \overline{\delta}^2}{c_g \mu k_c K} \left[\frac{\rho g \overline{\delta}}{3} - \frac{\gamma}{2} \right] + \frac{\overline{Y}_{A0}}{K} \tag{9}$$

DESCRIPTION OF THE PERTURBED SYSTEM

The formal description of the perturbed system is closely analogous to that of Ludviksson and Lightfoot, and the formal expressions for the velocity profiles are identical. Only a summary of these latter will be given here. We again assume all perturbations to be independent of z and to have the general form

$$W = \overline{W} + W'$$

$$W' = W(\eta) e^{i\alpha\xi} e^{\beta\tau}$$

where W is any one of the independent variables. The overline and prime represent the unperturbed value of W and the perturbation, respectively, and $W(\eta)$ is a function to be determined. For the special case of the film thickness $\delta^{*\prime}$, we write

$$\delta^{*\prime} = \frac{b_0}{\delta} e^{i\alpha\xi} e^{\beta\tau}$$

We will concern ourselves here primarily with the case of neutral stability for which $\beta = 0$ and will not consider the possibility of oscillatory disturbances.

The η-dependent portions of the velocity profiles take the form

$$V_y(\eta) = \frac{\sigma}{4\mu\overline{V}_0} \frac{b_0}{\overline{\delta}} \frac{\alpha^2}{\sinh\alpha} \left[\alpha\eta\cosh\alpha\eta - \sinh\alpha\eta - \left(\frac{\alpha}{\tanh\alpha} - 1\right)\eta\sinh\alpha\eta \right] \tag{10}$$

$$V_x(\eta) = \frac{\sigma}{4\mu\overline{V}_0} \frac{b_0}{\overline{\delta}} \frac{\alpha}{\sinh\alpha} \left[\alpha^2\eta\sinh\alpha\eta - \left(\frac{\alpha}{\tanh\alpha} - 1\right)(\alpha\eta\cosh\alpha\eta + \sinh\alpha\eta) \right] \tag{11}$$

$$V_z(\eta) = -\frac{\overline{\delta} b_0 \rho g}{\mu V_0 \alpha \cosh\alpha} \sinh\alpha\eta \tag{12}$$

In these equations the same free surface boundary conditions have been used as in the paper of Ludviksson and Lightfoot, but as in that paper we have not yet satisfied the divergence of the surface equation of motion

$$\frac{1}{\mu\overline{V}_0} \nabla_{\pi}{}^{*}\sigma = \frac{\partial^2 V_y{}^{*\prime}}{\partial\xi^2} + \frac{\partial^2 V_y{}^{*\prime}}{\partial\zeta^2} - \frac{\partial^2 V_y{}^{*\prime}}{\partial\eta^2} \tag{13}$$

For this we need the perturbed concentration profile to get the dependence of σ on position.

PERTURBED CONCENTRATION PROFILE

The continuity equation for the concentration perturbation is

$$(D^2 - \alpha^2) X_A(\eta) = \frac{\overline{\delta}\overline{V}_0}{\mathcal{D}_{AL}} \left(\frac{\partial \overline{X}_A}{\partial \eta} V_y(\eta) + \overline{\delta}\,\overline{G}_0 V_z(\eta) \right) = F(\eta) \tag{14}$$

This equation can be rewritten with the aid of Equations (9), (10), and (12) to obtain

$$F(\eta) = \overline{G}_0 b_0 \left(\frac{\alpha^2}{4N_{Cr}\sinh\alpha}\right) \left\{ \left[\left(\frac{N_{Ma}}{2} - \frac{N_d}{2}\right)\eta^2 + \frac{N_d}{6}\eta^3 \right] \cdot [\alpha\eta\cosh\alpha\eta - \sinh\alpha\eta - S\eta\sinh\alpha\eta] - \frac{4}{\alpha^3} N_{Cr} N_d \tanh\alpha\sinh\alpha\eta \right\} \tag{15}$$

where

$$S = \frac{\alpha}{\tanh \alpha - 1}$$

and the dimensionless groups

$$N_{Ma} = \frac{\gamma \bar{\delta}^2}{\mu \mathcal{D}_{AL}} = \frac{\Gamma \bar{G}_0 \bar{\delta}^2}{\mu \mathcal{D}_{AL}}, \quad N_{Cr} = \frac{\mu \mathcal{D}_{AL}}{\sigma \bar{\delta}},$$

$$N_d = \frac{\rho g \bar{\delta}^3}{\mu \mathcal{D}_{AL}} = N_{Fr} N^2_{Re} N_{Sc}, \quad N_{Fr} = \frac{g\bar{\delta}}{\bar{V}_0^2},$$

$$N_{Re} = \frac{\rho \bar{\delta} \bar{V}_0}{\mu}, \quad N_{Sc} = \frac{\mu}{\rho \mathcal{D}_{AL}}.$$

Two boundary conditions needed for the solution of the above differential equation are

$$\text{At } \eta = 0 \quad DX_A(\eta) = 0 \tag{16}$$

$$\text{At } \eta = 1 \quad DX_A + RX_A + b_0 \bar{G}_0 \left[N_{Ma} - \frac{N_d}{2} \right] + Rb_0 \bar{G}_0 \left[\frac{N_{Ma}}{2} - \frac{N_d}{3} \right] = 0 \tag{17}$$

where $R = (k_c K \bar{\delta} / \mathcal{D}_{AL})$. The first boundary condition comes from the fact that there is no mass flux across the solid wall. The second boundary condition is based on the assumption that the gas-phase concentration remains undisturbed. This is physically realistic if we are considering only localized instabilities and is reasonable for this preliminary analysis. Equation (17) is obtained by expanding the expression for interfacial mass flux about the position $\eta = 1$ in a Taylor series and neglecting the second- and high-order terms. The solution of Equation (14) can now be easily found. It takes the form

$$X_A(\eta) = G_0 b_0 \frac{\alpha^2}{4 N_{Cr} \sinh \alpha} [(A + D\eta^5 + F\eta^4 + H\eta^3 + J\eta^2 + L\eta) \cosh \alpha\eta + (B + C\eta^5 + E\eta^4 + G\eta^3 + I\eta^2 + K\eta) \sinh \alpha\eta] \tag{18}$$

where

$$A = -\frac{1}{R + \alpha \tanh \alpha} \Big\{ [(5C + 4E + 3G + 2I + K) + \alpha (D + F + H + J + L) + R(B + C + E + G + I + K)] \tanh \alpha + [(5D + 4F + 3H + 2J + L) + \alpha(B + C + E + G + I + K) + R(D + F + H + J + L)] + \frac{4}{\alpha^2} \tanh \alpha \left(1 + \frac{R}{2}\right) N_{Cr} N_{Ma} - \frac{4}{\alpha^2} \tanh \alpha \left(\frac{1}{2} + \frac{R}{3}\right) N_{Cr} N_d \Big\}$$

$$B = \left(\frac{S}{8\alpha^6} - \frac{5}{16\alpha^4} + \frac{2}{\alpha^5} N_{Cr} \tanh \alpha \right) N_d + \frac{5}{16\alpha^4} N_{Ma}$$

$$C = \frac{1}{60} N_d$$

$$D = -\frac{S}{60\alpha} N_d$$

$$E = \left(\frac{S}{24\alpha^2} - \frac{1}{16} \right) N_d + \frac{1}{16} N_{Ma}$$

$$F = \left(\frac{S}{16\alpha} - \frac{1}{16\alpha} \right) N_d - \frac{S}{16\alpha} N_{Ma}$$

$$G = \left(\frac{1}{8\alpha^2} - \frac{S}{8\alpha^2} \right) N_d + \frac{S}{8\alpha^2} N_{Ma}$$

$$H = \left(\frac{5}{24\alpha} - \frac{S}{12\alpha^3} \right) N_d - \frac{5}{24\alpha} N_{Ma}$$

$$I = \left(\frac{S}{8\alpha^4} - \frac{5}{16\alpha^2} \right) N_d + \frac{5}{16\alpha^2} N_{Ma}$$

$$J = \left(\frac{3S}{16\alpha^3} - \frac{3}{16\alpha^3} \right) N_d - \frac{3S}{16\alpha^3} N_{Ma}$$

$$K = \left(\frac{3}{16\alpha^4} - \frac{3S}{16\alpha^4} \right) N_d + \frac{3S}{16\alpha^4} N_{Ma}$$

$$L = \left(\frac{5}{16\alpha^3} - \frac{S}{8\alpha^5} - \frac{2}{\alpha^4} N_{Cr} \tanh \alpha \right) N_d - \frac{5}{16\alpha^3} N_{Ma}$$

THE CHARACTERISTIC EQUATION

Equations (10), (11), (12), and (18) express the velocity and concentration perturbations as functions of the physical properties and flow conditions, via the governing dimensionless ratios, for any α at neutral stability. It remains, however, to satisfy the divergence of the surface equation of motion, Equation (13), which has not yet been used. It can be written as

$$X_A(\eta)|_{\eta=1} + b_0 \bar{G}_0 \left[N_{Ma} \frac{\eta^2}{2} - N_d \left(\frac{\eta^2}{2} - \frac{\eta^3}{6} \right) \right] \Bigg|_{\eta=1} = \frac{\mu \bar{V}_0}{\Gamma \alpha^2} (D^2 + \alpha^2) V_y(\eta)|_{\eta=1} \tag{19}$$

with the assumption of linear dependence of surface tension on concentration [see Equation (5)] and the assumed forms of the perturbations. This equation is also obtained by expanding each term at the interface about $\eta = 1$ and neglecting second- and higher-order terms. Use of this equation completes the characteristic value problem and gives the conditions of neutral stability for any α. Substituting Equations (10) and (18) into Equation (19), we obtain

$$(B + C + E + G + I + K) \tanh^2 \alpha + (A + D + F + H + J + L) \tanh \alpha + \frac{\tanh^2 \alpha}{\alpha^2} N_{Cr} \left(2N_{Ma} - \frac{4}{3} N_d \right) = \frac{2}{N_{Ma}} \left[\frac{\tanh \alpha}{\alpha} + \frac{1}{\cosh^2 \alpha} \right] \tag{20}$$

With the aid of expressions for the coefficients, A, B, C, etc., and after a considerable algebraic rearrangement, we can show that the final form of the characteristic equation for neutral stability is

$$N_{Ma}^2 [(-15\alpha^6 - 45\alpha^4 - 30\alpha^2) \tanh^3 \alpha + (30\alpha^5 + 15\alpha^3 - 45\alpha) \tanh^2 \alpha + (15\alpha^6 + 45\alpha^4 + 90\alpha^2) \tanh \alpha + (-30\alpha^5 - 45\alpha^3)$$

$$+ 480\alpha^3 \tanh^2 \alpha\, N_{Cr}(2 - \alpha \tanh \alpha)\,]$$
$$+ N_{Ma}N_d\,[(11\alpha^6 + 25\alpha^4 + 15\alpha^2 + 30)\tanh^3 \alpha$$
$$+ (-20\alpha^5 + 5\alpha^3)\tanh^2 \alpha - (11\alpha^6 + 25\alpha^4 + 45\alpha^2)$$
$$\tanh \alpha + (20\alpha^5 + 15\alpha^3) - 480\alpha \tanh^4 \alpha\, N_{Cr}$$
$$+ 160\alpha^3 \tanh^2 \alpha\, N_{Cr}(-3 + 2\alpha \tanh \alpha)\,]$$
$$+ (R + \alpha \tanh \alpha)\left(480\alpha^4 \tanh \alpha - \frac{480\alpha^5}{\cosh^2 \alpha}\right) = 0 \qquad (21)$$

Equation (21) gives the loci of Marangoni numbers or surface-tension gradients for each α which bound the regions of instability, that is, the curves of marginal stability.

As expected, the unspecified amplitude of the disturbance b_0 has disappeared, and the characteristic equation is even in the wave number, hence independent of the sign of α.

The main difference between Equation (21) and the corresponding equation of Ludviksson and Lightfoot is that the last term contains R, which provides a measure of the relative importance of mass transfer resistance in the liquid and gas phases. We can anticipate that when gas-phase resistance is negligible and R approaches infinity, the system should always be stable since no lateral surface concentration differences can occur.

LOCI OF NEUTRALLY STABLE DISTURBANCES

We can now plot the loci of neutrally stable disturbances for given system properties and film thickness by solving Equation (21) for γ in terms of assumed real values of α. It is convenient to combine the dimensionless groups for the purpose of correlation. If we choose to work with a dimensionless surface-tension gradient defined as

$$\gamma^0 = \gamma/\sqrt{\rho g \sigma} = N_{Ma}\sqrt{N_{Cr}/N_d}$$

Equation (21) can be rewritten in the form

$$a\gamma^{02} + b\gamma^0 + c = 0$$

Here the coefficients a, b, and c are functions of the dimensionless film thickness $\delta^0 = \bar{\delta}\sqrt{\rho g/\sigma} = \sqrt{N_{Cr}N_d}$, a physical property ratio $N_p = \mu^2\mathcal{D}_{AL}{}^2\rho g/\sigma^3 = N_d N_{Cr}{}^3$, R the ratio of liquid to gas-phase mass transfer resistance and the dimensionless wave number α.

The form of the relation between γ^0 and α is shown in Figure 2 for representative values of the governing parameters. The physical properties used for the construction of these curves are typical of common organic mixtures. It should be noted that both positive and negative surface-tension gradients are displayed here and that unstable regions are predicted for both.

From Figure 2 we see that for sufficiently thin films and long wavelengths of disturbances, the behavior is qualitatively similar to that obtained by Ludviksson and Lightfoot for the case of heat transfer; that is, the marginal stability curves (1*a* or 2*a*) form a closed region with instabilities predicted inside it and stable operations predicted for sufficiently high or sufficiently low positive surface-tension gradients. No unstable region is found for negative surface-tension gradients at these low α. This type of behavior occurs where $\alpha < \alpha_c$, the wave number for which the instabilities begin to be predicted for negative surface-tension gradients.

At shorter wavelengths of disturbances ($\alpha > \alpha_c$) additional marginal stability curves (1*b*, 1*c* or 2*b*, 2*c*) are found for the same system properties and film thickness. As α approaches α_c the γ^0 of marginal stability approaches a positive limiting value $\gamma^0 = -b/c$ for the upper curve and negative infinity for the lower curve. Proceeding from the known stable region on the left without crossing a marginal stability curve, one finds that the stable region is between these curves while unstable regions are those above and below. Thus we have three distinct unstable regions and one continuous stable region for thinner films.

As the film thickness increases, the apex of the closed region (curves marked with *a*) approaches α_c and eventually merges with the curves marked with *b*. At this point the upper curve of 3*a* goes to infinity but the lower curve of 3*a* forms a continuous curve with 3*b* with $\gamma_c{}^0 = -b/c$ at α_c. Now there are two separate stable regions and two unstable regions.

The physical interpretation of these curves is not obvious. For low α the arguments are the same as those of Ludviksson and Lightfoot; that is, we don't expect instability for negative surface-tension gradients since a thickening in the film leads to a roll cell or rivulet with low surface-tension in the crest and hence disturbances will be dissipated. For low positive surface-tension gradients the concentration increase in the crest is dissipated fast enough to prevent the instability. For very high surface-tension gradients the net flow is upward and an increase in thickness leads to a rivulet which is representative of downstream conditions, that is, low surface tension; hence the system is stable. It should be kept in mind, however, that these conditions of net upward flow are not consistent with the physical system modeled, which assumes countercurrent flow, and hence are of limited interest. For moderate surface-tension gradients, instability is possible.

For $\alpha > \alpha_c$ the situation is more complicated. In fact, the situation seems to have been completely reversed as

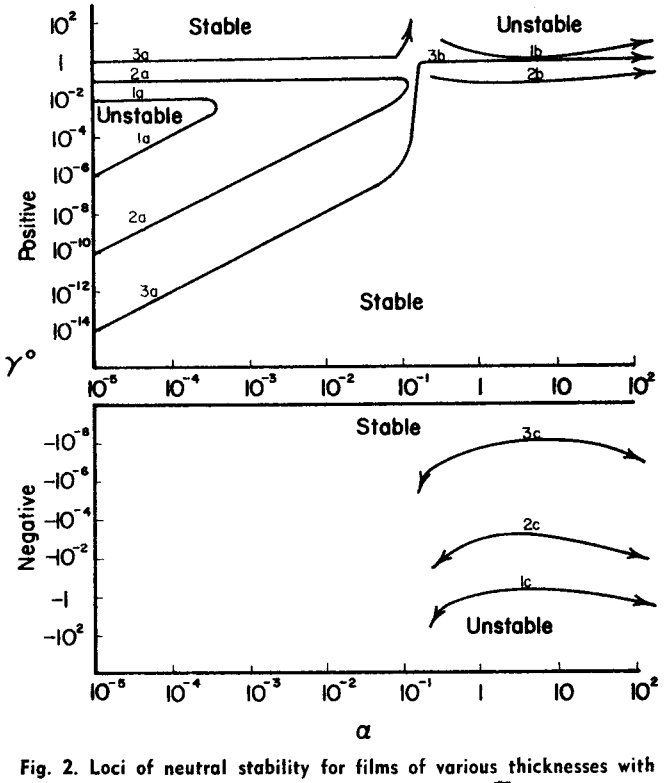

Fig. 2. Loci of neutral stability for films of various thicknesses with $Np = 2.69 \times 10^{-14}$ and $R = 300$ (Curve 1: $\bar{\delta} = 10^{-3}$ cm., $\bar{\delta} = 6.76 \times 10^{-3}$; Curve 2: $\bar{\delta} = 10^{-2}$ cm., $\delta^0 = 6.76 \times 10^{-2}$ cm.; Curve 3: $\delta + 10^{-1}$ cm., $\delta\ 6.76 \times 10^{-1}$).

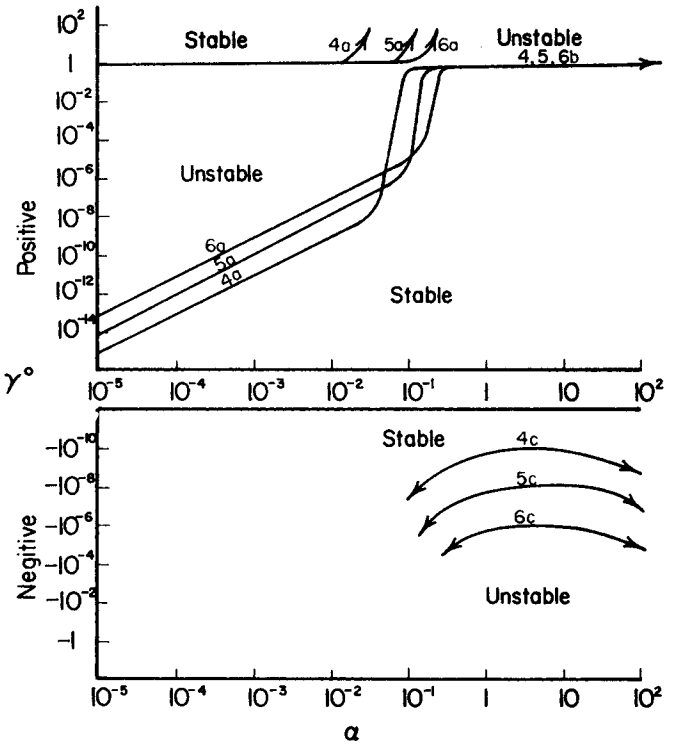

Fig. 3. Effect of physical property ratio Np with $R = 300$ and $\delta^0 = 6.76 \times 10^{-2}$ (Curve 4: $Np = 2.49 \times 10^{-16}$; Curve 5: $Np = 2.49 \times 10^{-14}$; Curve 6: $Np = 2.49 \times 10^{-12}$).

we now have unstable regions for very large positive and negative γ^0 but a stable region in between. The apparent explanation of this behavior is that when the wavelengths of disturbances are small, lateral diffusion (in the x direction) becomes important; that is, at short wavelengths sharp lateral concentration gradients are formed and solute in the interior of faster flowing ridges diffuses to a nearby trough while the surface of the ridge is maintained in more effective equilibrium with the gas phase than the surface of the trough. This can eventually cause a crossover in the concentration profile for $\alpha \geq \alpha_c$ even though the crest of the ridge is of higher surface tension than the trough. This situation can be verified by calculating the perturbed surface concentration, or, more conveniently, by considering the difference between perturbed and unperturbed surface concentrations as a function of α, that is

$$X_A|_{\eta=1+\delta^*1} - \overline{X}_A|_{\eta=1} = g(\alpha)$$

The sign of $g(\alpha)$ determines whether the crest surface has a lower or higher concentration than the unperturbed state. The case for which $g(\alpha) = 0$ determines γ^0 as a function of α at which no lateral surface concentration gradient can develop. The relation between γ^0 and α for $g = 0$ is very similar to the curve of marginal stability. At low α the relation for $g = 0$ coincides with curve 3*a* of Figure 2, as expected. For large α it coincides with curve 3*b*. In between there is a point of discontinuity which we will call the critical crossover wave number α_c, where the stability characteristics seem to reverse. It is found that α_c is a very weak function of film thickness as well as physical properties and mass transfer characteristics R.

In addition to these features we should note from Figure 2 that as the film thickness increases the unstable region increases, which is in agreement with the results of Ludviksson and Lightfoot. From Figure 3 the unstable regions shrink as the physical property ratio N_p increases, indicating that liquid films of higher viscosity and higher diffusivity are more stable. This again is expected on intuitive grounds and agrees with other analyses of film stability. From Figure 4 it is seen that an increase in R tends to shrink the unstable regions, again as expected, because a higher mass transfer coefficient for the gas phase rela-

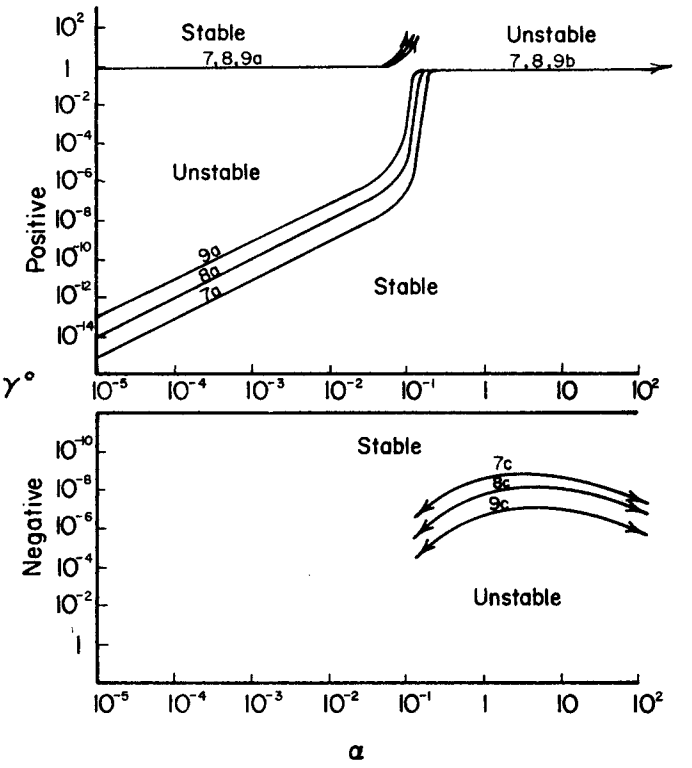

Fig. 4. Effect of mass transfer characteristics R with $Np = 2.49 \times 10^{-14}$ and $\delta^0 = 6.76 \times 10^{-2}$ (Curve 7: $R = 30$; Curve 8: $R = 300$; Curve 9: $R = 3000$).

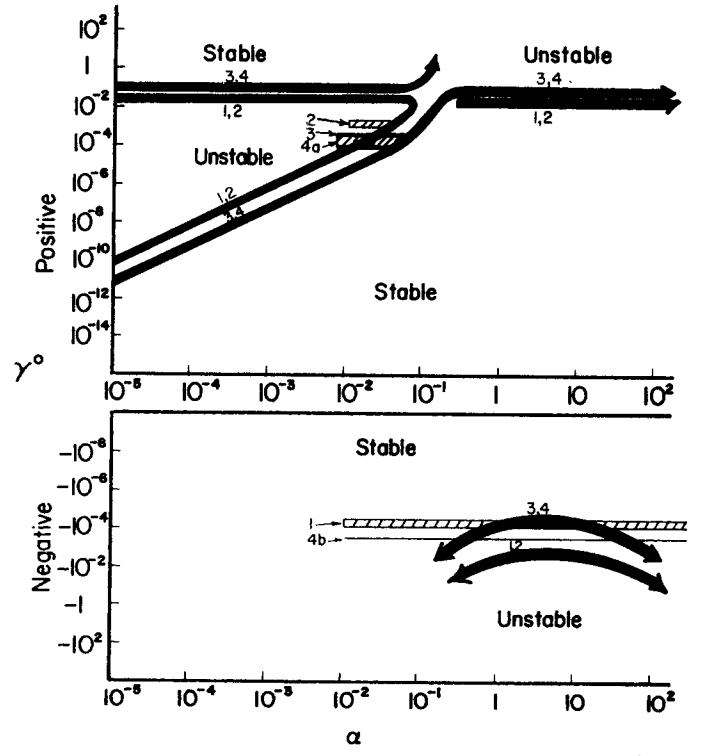

Fig. 5. Comparison of the analysis with semiquantitative data obtained by Zuiderweg and Harmens.

tive to liquid conductance means that the interface is more nearly in equilibrium with the gas phase. Hence the lateral concentration gradients and the resulting surface-tension gradients are depressed.

It now remains to assess the importance of these results for real systems. First we note that very high upward surface-tension gradients require net upward flow in the film. This is inconsistent with our model and of little or no practical interest. Since the surface-tension gradient required for zero net flow of the liquid film is usually below the upper part of the neutral stability curve, these regions of very high upward surface-tension gradients are not important to us.

The semiquantitative data obtained by Zuiderweg and Harmens can be compared with our analysis. Their data and the corresponding characteristic curves are plotted in Figure 5. Note we are making use of average physical properties of the system investigated and assume surface tension to be a linear function of the surface concentration. The equilibrium data are obtained from Chu (*13, 14*).

The experimental systems with upward directed surface-tension gradients reported by Zuiderweg and Harmens include regions of unstable α according to our analysis. Under these conditions instabilities were always actually observed in agreement with our prediction. These data are indicated in Figure 5 by the cross-shaded areas 2, 3, and 4*a*. From geometrical consideration we have the restriction $\lambda < \pi D$, where D is the diameter of the column. Recall α is defined as $2\pi\bar{\delta}/\lambda$; hence the possible minimum wave number of disturbances is $2\bar{\delta}/D$ corresponding to the left limit of the shaded areas. Following this argument it seems then possible to reduce instabilities by reducing the perimeter of the film supports; this is reasonable on intuitive grounds. However, the data in Figure 5 indicate that in order to get out of the unstable region completely α must be greater than 0.1, that is, $D < 20\,\bar{\delta}$. For $\bar{\delta} = 0.01$ cm. this is on the order of 0.2 cm., which is too small for practical systems. One should also notice that if $\bar{\delta}$ and D are of comparable size, then the curvature effect may become important.

For systems of negative γ^0 we find most of the data in agreement with our analysis as indicated by the shaded area in Figure 5. Here no instabilities are predicted and none observed. However there is one experimental datum point reported for which we predict possible instability over a limited range of α's while the experiment seems to indicate stable operation. This disagreement, however, is not necessarily conclusive because the growth constant β which we have not considered may be too small for the instability to be observed, or to have effect on the HETP reported by Zuiderweg and Harmens. It is also possible that differences between actual operating conditions and these postulated in our model are important.

Instabilities corresponding to the case of negative surface-tension gradients have not been reported to our knowledge, and experimental data are needed to test this aspect of our results.

In view of the highly idealized nature of our analysis, further improvement of it may be necessary, such as consideration of thermal effects (combined heat and mass transfer). Furthermore, experiments must be designed specifically to conform with our assumptions before our results can be tested conclusively. This simplified analysis, however, has given us some insight into the instabilities of the type commonly observed in mass transfer operations, and makes semiquantitative estimates of stability conditions possible. It may thus prove useful in designing for conditions favorable to mass transfer efficiency.

NOTATION

a, b, c = constants of the characteristic equation, Equation (21), written as a quadratic in dimensionless surface-tension gradients
b_0 = unspecified infinitesimal disturbance on film thickness, cm.
$\bar{c}_L, \bar{c}_g$ = total concentration of the liquid film and gas phase, respectively, mole/liter
D = $\partial/\partial\eta$
= diameter of the column, cm.
$\mathcal{D}_{AL}$ = mass diffusivity in liquid phase, sq.cm./sec.
g = gravitational acceleration, cm./sec.^{2}
$\bar{G}_0$ = unperturbed axial concentration gradient
i = imaginary index
K = vapor-liquid equilibrium constant
k_c = local gas-phase mass transfer coefficient
N_{Ay} = interfacial mass flux
$N_{Cr} = \mu\mathcal{D}_{AL}/\sigma\bar{\delta}$ = Crispation number
$N_d = \rho g\bar{\delta}^3/\mu\mathcal{D}_{AL} = N_{Fr}N_{Re}^2N_{Sc}$ = dimensionless number
$N_{Fr} = g\bar{\delta}/\bar{V}_0^2$ = Froude number
$N_{Ma} = \gamma\bar{\delta}^2/\mu\mathcal{D}_{AL}$ = Marangoni number
$N_{Re} = \rho\bar{\delta}\bar{V}_0/\mu$ = Reynolds number
$N_{Sc} = \mu/\mathcal{D}_{AL}\rho$ = Schmidt number
$N_p = \mu^2\mathcal{D}_{AL}^2\rho g/\sigma^3 = N_dN_{Cr}^3$ = physical property group
$R = \bar{c}_g k_c K\bar{\delta}/\mathcal{D}_{AL}\bar{c}_L$
$\bar{V}_0$ = arbitrary reference velocity, cm./sec.
$\bar{V}_x, \bar{V}_y, \bar{V}_z$ = unperturbed velocity components, cm./sec.
$\bar{V}_x(\eta), \bar{V}_y(\eta), \bar{V}_z(\eta)$ = functional dependence of dimensionless perturbed velocity components on η
$V_y^{*\prime}$ = dimensionless perturbed velocity component in y direction
W = any one of the independent variables
$\bar{W}$ = unperturbed value of W
W' = perturbed value of W'
$W(\eta)$ = functional dependence of perturbed W on η
x, y, z = Cartesian coordinates, cm.
$\bar{X}_A$ = unperturbed concentration profile (mole fraction)
$X_A(\eta)$ = functional dependence of dimensionless perturbed concentration on η
$\bar{Y}_A$ = unperturbed gas-phase concentration profile (mole fraction)
$\bar{Y}_{A0}$ = arbitrary gas-phase reference concentration

Greek Letters

$\alpha = 2\pi\bar{\delta}/\lambda$ = dimensionless wave number
α_c = crossover wave number
β = complex growth constant, sec.$^{-1}$
γ = surface-tension gradient, dyne/sq.cm.
$\gamma^0 = \gamma/\sqrt{\rho g\sigma}$ = dimensionless surface-tension gradient
γ_c^0 = value of γ^0 at α_c
$\bar{\delta}$ = unperturbed film thickness, cm.
$\delta^{*\prime}$ = dimensionless perturbation on film thickness
$\delta^0 = \bar{\delta}\sqrt{\rho g/\sigma}$ = dimensionless film thickness
∇_π^* = dimensionless two-dimensional gradient vector in surface coordinates (x, z)
ρ = density, g./cu.cm.
μ = viscosity, poise
σ = surface tension, dyne/cm.
Γ = concentration coefficient of surface tension
$\xi = x/\bar{\delta}$
$\eta = y/\bar{\delta}$ = dimensionless Cartesian coordinates

$\zeta = z/\bar{\delta}$

τ = dimensionless time

LITERATURE CITED

1. Ludviksson, V., and E. N. Lightfoot, *AIChE J., 14,* 620 (1968).
2. Zuiderweg, F. J., and A. Harmens, *Chem. Eng. Sci.*, 9, 89 (1958).
3. Francis, R. C., and J. C. Berg, *ibid.*, 22, 685 (1967).
4. Brian, P. L. T., J. E. Vivian, and D. C. Matiatos, *AIChE J.*, 13, 28 (1967).
5. Banerjee, S., E. Rhodes, and D. S. Scott, *Chem. Eng. Sci.*, 22, 43 (1967).
6. Emmert, R. E., and R. L. Pigford, *ibid.*, 2, 87 (1954).
7. Molstad, M. C., and L. F. Parsley, *ibid.*, 46, 20 (1950).
8. Norman, W. S., and B. K. Soloman, *Trans. Inst. Chem. Eng.*, 37, 237 (1959).
9. Bond, J., and M. B. Donald, *Chem. Eng. Sci.*, 6, 237 (1967).
10. King, P. J., and P. N. Walmsley, *J. Appl. Chem.*, 15, 98 (1965).
11. Sternling, C. V., and L. E. Scriven, *AIChE J.*, 6, 514 (1959).
12. Chu, J. C., S. L. Wang, S. L. Levy, and R. Paul, "Vapor-Liquid Equilibrium Data," J. W. Edwards, Ann Arbor, Mich. (1956).
13. Chu, J. C., R. J. Getty, L. F. Brennecke, and R. Paul, "Distillation Equilibrium Data," Rheinhold, New York (1950).

Manuscript received September 10, 1968; revision received March 25, 1971; paper accepted April 5, 1971.

An Experiment on Turbulent Diffusion in Additive Solutions

JIN WU

Hydronautics, Inc., Laurel, Maryland

Turbulent diffusion in high molecular weight additive solutions was measured and compared on a laboratory scale by observing the axisymmetric spreading of a cylindrical turbulent cloud in these solutions of various concentrations. Significant suppression of turbulence in additive solutions was observed. The trend of the results as a function of additive concentrations is similar to that of the additive reduction of turbulent frictional resistance.

The reduction of turbulent friction experienced by pumping additive solutions through pipes (*6*) seems to indicate the suppression of turbulence. However, it is held (*3, 10*) that these additive effects occur only in the region very close to the wall where the shear strain is high and the turbulence scale is small. These effects lead to a thickening of the viscous sublayer and consequently result in drag reduction. This argument, additive effects occurring only in the wall region, might discourage studies on free turbulent flow of additive solutions. However, the greatly suppressed advance of a turbulent front in additive solutions (*4, 11*) seems to evidence additive effects on turbulent diffusion. The present article includes the previously unpublished study (*11*) on the generation and the spreading of an axisymmetric, turbulent region in additive solutions. This result is important for estimating the diffusion of additive solutions ejected into a turbulent pure-water boundary layer.

EQUIPMENT AND EXPERIMENTAL TECHNIQUES

The turbulent cloud was generated by a spiral paddle in a transparent tank, 3 m. deep, 3 m. long, and 23 cm. wide. The paddle, shown in Figure 1*a*, was made by soldering screen sections to a rigid spiral frame, 5 cm. in diameter. Supported by a 0.9-cm. diam. perforated tube shaft, the paddle was connected to and controlled by a pendulum arrangement behind the tank. The paddle rotated about its axis as the pendulum swung outside the tank. Immediately prior to the test, a dye rod was inserted into a perforated tube. In several minutes the dye started to dissolve, and by then the turbulence created by the insertion of the dye rod was damped. The turbulent cloud was generated then by the spiral paddle with the pendulum swinging for a complete cycle, through a repeatable arc of 240 deg. The pendulum was released from the same position for all the tests and was caught on its back swing. The period of the generation is about 2 sec. With the help of dye being dissolved continuously into the cloud during the spreading process, the cloud boundary, although irregular, was distinctly visible, and was photographed by a movie camera. The cross section of the cylindrical cloud, during this photographing period (about 30 sec.), was radially symmetric generally; see Figure 1*b*. The radially symmetric shape indicates that an axisymmetrical flow is generated. The dark column shown in Figure 1*b* below the cloud was not generated by the paddle but was left there by dye dissolved from the dye rod.

In the present experiment, aqueous solution of polyox (polyethylene oxide, WSR-301) was selected as the testing medium. The concentrations for this additive were varied between 0 and 1,250 p.p.m.w.

This experimental technique was designed for studying, on a comparative basis, the turbulence-diffusion characteristics of additive solutions by observing the generation of a cylindrical turbulent cloud and its spreading in these solutions. During the generating process, large-scale eddies, having sizes comparable to the diameter of the paddle, were created by the frame of the paddle, while smaller ones, having sizes comparable to the void of the screen, were also excited. The total circulation introduced by the forward and backward swing of the paddle was virtually nil.

RESULTS

The process of diffusion of a cylindrical turbulent cloud in an undisturbed fluid consists of two different effects: